

This discussion paper is/has been under review for the journal *Atmospheric Chemistry and Physics (ACP)*. Please refer to the corresponding final paper in *ACP* if available.

**Aerosol
hygroscopicity
closure using AMS
and DASH-SP data**

S. P. Hersey et al.

Aerosol hygroscopicity in the marine atmosphere: a closure study using high-resolution, size-resolved AMS and multiple-RH DASH-SP data

S. P. Hersey, A. Sorooshian, S. M. Murphy, R. C. Flagan, and J. H. Seinfeld

Departments of Chemical Engineering and Environmental Science and Engineering, Caltech, 1200 E. California Blvd, Pasadena, CA, 91125, USA

Received: 14 July 2008 – Accepted: 6 August 2008 – Published: 4 September 2008

Correspondence to: J. H. Seinfeld (seinfeld@caltech.edu)

Published by Copernicus Publications on behalf of the European Geosciences Union.

Title Page

Abstract

Introduction

Conclusions

References

Tables

Figures

⏪

⏩

◀

▶

Back

Close

Full Screen / Esc

Printer-friendly Version

Interactive Discussion

Abstract

We have conducted the first closure study to couple high-resolution aerosol mass spectrometer (AMS) composition data with size-resolved, multiple-RH, high-time-resolution hygroscopic growth factor (GF) measurements from the differential aerosol sizing and hygroscopicity spectrometer probe (DASH-SP). These data were collected off the coast of Central California during seven of the 16 flights carried out during the MASE-II field campaign in July 2007. Two of the seven flights were conducted in airmasses that originated over the continental United States. These flights exhibited elevated organic volume fractions ($VF_{\text{organic}}=0.46\pm0.22$, as opposed to 0.24 ± 0.18 for all other flights), corresponding to significantly suppressed GF s at high RH (1.61 ± 0.14 at 92% RH, as compared with 1.91 ± 0.07 for all other flights), more moderate GF suppression at intermediate RH (1.53 ± 0.10 at 85%, compared with 1.58 ± 0.08 for all other flights, and no measurable GF suppression at low RH (1.31 ± 0.06 at 74%, compared with 1.31 ± 0.07 for all other flights). Organic loadings were slightly elevated in above-cloud aerosols, as compared with below-cloud aerosols, and corresponded to a similar trend of significantly suppressed GF at high RH, but more moderate impacts at lower values of RH. A hygroscopic closure based on a volume-weighted mixing rule provided excellent agreement with DASH-SP measurements ($R^2=0.79$). Minimization of root mean square error between observations and predictions indicated mission-averaged organic GF s of 1.20, 1.43, and 1.46 at 74, 85, and 92% RH, respectively. These values agree with previously reported values for water-soluble organics such as dicarboxylic and multifunctional acids, and correspond to a highly oxidized, presumably water-soluble, organic fraction (O:C=0.92±0.33). Finally, a backward stepwise linear regression revealed that, other than RH, the most important predictor for GF is VF_{organic} , indicating that a simple empirical model relating GF , RH, and the relative abundance of organic material can provide accurate predictions of hygroscopic growth in the marine atmosphere.

Aerosol hygroscopicity closure using AMS and DASH-SP data

S. P. Hersey et al.

Title Page

Abstract

Introduction

Conclusions

References

Tables

Figures

⏪

⏩

◀

▶

Back

Close

Full Screen / Esc

Printer-friendly Version

Interactive Discussion



1 Introduction

Atmospheric aerosols change size with fluctuations in relative humidity, with a magnitude dictated by chemical composition. Because this hygroscopic response determines particle size, it influences direct climate forcing attributed to aerosols. Further, sub-saturated hygroscopic growth factor ($D_{p,wet}/D_{p,dry}$) is strongly correlated with CCN activity (Prenni et al., 2001). Given the importance of aerosol water uptake on both the direct and indirect light scattering properties of aerosols, incomplete understanding of aerosol hygroscopicity has been identified as a major limitation in estimations of climate forcing (IPCC, 2007).

With a firm foundational understanding of hygroscopic properties of inorganic aerosol constituents, there has been a significant shift in focus toward organic hygroscopicity in the last decade, as a number of theoretical (e.g., Clegg and Seinfeld, 2006; Topping et al., 2005a,b), laboratory (Peng et al., 2001; Choi and Chan, 2002a; Peng and Chan, 2001; Choi and Chan, 2002b; Sjogren et al., 2007; Virkkula et al., 1999; Cruz and Pandis, 2000; Prenni et al., 2001; Cocker et al., 2001a,b; Hameri et al., 2002; Saathoff et al., 2003; Prenni et al., 2003; Petters et al., 2006; Varutbangkul et al., 2006; Sjogren et al., 2007; Prenni et al., 2007; Moore and Raymond, 2008; Rood et al., 1985; Carrico et al., 1998, 2000; Dougle et al., 1998; Magi and Hobbs, 2003; Kim et al., 2006; Kreisberg et al., 2001; Hegg et al., 2006; Massling et al., 2007), and chamber (e.g., Ansari and Pandis, 2000; Cocker et al., 2001a,b; Duplissy et al., 2008) studies have sought to address how the presence of organics affects the water uptake characteristics of atmospheric aerosol. Despite advances in understanding hygroscopic characteristics of organic-containing aerosols, measurements of aerosol hygroscopicity in field campaigns have remained relatively sparse.

Closure studies, which attempt to reconcile simultaneously measured hygroscopic and chemical data, link laboratory studies of hygroscopicity, theoretical models for water uptake, and field measurements of aerosol-water interactions. The standard method for predicting hygroscopic growth from composition data is based on volume-

Aerosol hygroscopicity closure using AMS and DASH-SP data

S. P. Hersey et al.

Title Page

Abstract

Introduction

Conclusions

References

Tables

Figures



Back

Close

Full Screen / Esc

Printer-friendly Version

Interactive Discussion

weighted water uptake by the individual chemical constituents. While it is usually possible to predict water uptake for the inorganic fraction of atmospheric aerosols, the wealth of organic species in the atmosphere, combined with limited understanding of organic aerosol hygroscopicity, has led investigators to assign the water uptake of organics as the particle growth not explained by inorganic constituents (e.g., Malm et al., 2005).

An important approach in hygroscopicity closure is to represent organics as a combination of water-soluble and insoluble fractions, corresponding to oxygenated (OOA) and hydrocarbon-like (HOA) carbon, respectively. One notable study in an urban atmosphere (Gysel et al., 2007) used high-resolution chemical data from the aerosol mass spectrometer (AMS, Jayne et al., 2000) to separate the organic component into OOA and HOA by using m/z 44 and 57 signals, respectively, with a deconvolution method developed by Zhang et al. (2005). In the study, division of organics between hygroscopically active and inactive fractions provided good agreement between predicted and measured hygroscopicity values. This study represents an improvement in the hygroscopic treatment of organics over prior work, but applies only to urban aerosol and is limited by both low time resolution and single-RH conditions inherent in HTDMA systems.

The current study presents data obtained during seven flights in the marine atmosphere off the coast of Central California during the second Marine Stratus/Stratocumulus Experiment (MASE-II). The dataset is the first to combine high-time-resolution, size-resolved AMS chemistry with high-time-resolution, size-resolved hygroscopic data at multiple RH values from the Differential Aerosol Sizing and Hygroscopicity Spectrometer Probe (DASH-SP). Hygroscopic studies have previously been carried out in the marine atmosphere (see Table 1), but none with chemical and hygroscopic data as highly size-, time-, and RH-resolved as those presented here.

Aerosol hygroscopicity closure using AMS and DASH-SP data

S. P. Hersey et al.

Title Page

Abstract

Introduction

Conclusions

References

Tables

Figures

⏪

⏩

◀

▶

Back

Close

Full Screen / Esc

Printer-friendly Version

Interactive Discussion

2 Experimental

2.1 MASE-II experiment

The data presented here were obtained during a series of seven cloud probing flights carried out as part of the second Marine Stratus/Stratocumulus Experiment (MASE-II) field campaign during July 2007. The MASE II experiment was the second of two airborne field campaigns directed toward measurement of aerosol-cloud relationships in marine stratocumulus in the eastern Pacific Ocean. The Marine Stratus/Stratocumulus Experiment (MASE) was carried out in 2005 off the coast of Monterey, California (Lu et al., 2007), and MASE II was undertaken in 2007 in the same region. Both experiments were carried out in the month of July, when marine stratocumulus are prevalent over the region, and utilized the CIRPAS Twin Otter aircraft. In each campaign, comprehensive airborne measurements were made of aerosol and cloud properties in areas both perturbed and unperturbed by local anthropogenic emissions. Tables 2 and 3 list the flights carried out during MASE II and the instrument payload onboard the Twin Otter, respectively. The present study addresses measurements of the hygroscopic properties of marine aerosols during MASE II. Other flights probed emissions from a large bovine source and a large container ship, and these data are presented elsewhere (Sorooshian et al., in preparation; Murphy et al., in preparation).

2.2 Aerosol composition measurements

Non-refractory aerosol chemical species were characterized by the Aerodyne compact Time of Flight Aerosol Mass Spectrometer (cToF-AMS, Drewnick et al., 2004a,b). In the AMS, particles with vacuum aerodynamic diameters ($D_{p,va}$) $50 \text{ nm} \leq D_{p,va} \leq 800 \text{ nm}$ are focused by an aerodynamic lens, pass through a 3.5% chopper, and are vaporized at 500°C . The chopper has three modes of operation, which detect background mass spectra, ensemble average mass spectra over all particle sizes, or size-resolved mass spectra. After vaporization, all molecules are ionized via electron impact, and undergo

Aerosol hygroscopicity closure using AMS and DASH-SP data

S. P. Hersey et al.

Title Page

Abstract

Introduction

Conclusions

References

Tables

Figures

⏪

⏩

◀

▶

Back

Close

Full Screen / Esc

Printer-friendly Version

Interactive Discussion

**Aerosol
hygroscopicity
closure using AMS
and DASH-SP data**

S. P. Hersey et al.

[Title Page](#)[Abstract](#)[Introduction](#)[Conclusions](#)[References](#)[Tables](#)[Figures](#)[⏪](#)[⏩](#)[◀](#)[▶](#)[Back](#)[Close](#)[Full Screen / Esc](#)[Printer-friendly Version](#)[Interactive Discussion](#)

time-of-flight mass analysis. In addition to sulfate, nitrate, and ammonium, the AMS detects total organic mass as a well-established sum of mass spectra. AMS data allows partitioning of organic species into oxygenated (OOA) and hydrocarbon-like (HOA) carbon with the use of m/z 44 and 57 markers, respectively, and a deconvolution method described by Zhang et al. (2005). Kondo et al. (2007) found that in aerosols collected in Tokyo, OOA and HOA correlated strongly with water-soluble organic carbon (WSOC) and water-insoluble organic carbon (WIOC), respectively, with nearly all WSOC being OOA and nearly all HOA being WIOC. These methods allow estimation of the fraction of aerosol comprised of WSOC and WIOC. Finally, O:C ratios are determined by using mass concentration at m/z 44 and a parameterization presented in Aiken et al. (2007).

AMS $D_{p,va}$ is converted to volume-equivalent diameter ($D_{p,ve}$) by assuming constant particle density of 1.65 g/cm^3 . Data represent size-resolved AMS chemistry, averaged over 10 nm size bins. Since hygroscopicity measurements were carried out for particles of dry electrical mobility diameter ($D_{p,em,dry}$) equal to 150, 175, and 200 nm, the corresponding AMS size bins were $145 \leq D_{p,ve} \leq 155 \text{ nm}$, $170 \leq D_{p,ve} \leq 180 \text{ nm}$, and $195 \leq D_{p,ve} \leq 205 \text{ nm}$, respectively.

2.3 Hygroscopicity measurements

Hygroscopicity measurements were carried out with the Differential Aerosol Sizing and Hygroscopicity Spectrometer Probe (DASH-SP, Brechtel Mfg; Sorooshian et al., 2008). Ambient particles pass through a nafion dryer before receiving a uniform charge distribution in a ^{210}Po neutralizer. A cylindrical, single-classification differential mobility analyzer (DMA) then size selects particles into narrow ranges of mobility-equivalent diameters ($D_{p,em}$) between 0.1 and 1.0 μm . The resulting monodisperse aerosol is split into five separate flows. One channel provides a redundant measurement of total particle concentration at the DMA-selected size with a water condensation particle counter (TSI Model 3831). The remaining four channels consist of parallel nafion humidification chambers (Perma Pure, LLP, Model MD-070-24FS-4), followed by cor-

Aerosol hygroscopicity closure using AMS and DASH-SP data

S. P. Hersey et al.

Title Page

Abstract

Introduction

Conclusions

References

Tables

Figures

◀

▶

◀

▶

Back

Close

Full Screen / Esc

Printer-friendly Version

Interactive Discussion



respondingly humidified custom optical particle counters (OPCs). In the OPC sample volume, particles pass through a focused laser beam ($\lambda=532$ nm, World Star Technologies, Model TECGL-30) and scatter light in proportion to size (D_p) and refractive index (RI). Forward-scattered light is collected and focused on a photomultiplier tube, and the resulting electrical pulse is recorded by a high-speed data acquisition computer. An iterative data processing algorithm, based on laboratory calibrations with salts of known refractive indices, is used to determine the best fit on a solution surface relating electrical pulse height, size, and refractive index. The hygroscopic growth factor ($GF=D_{p,wet}/D_{p,dry}$) is corrected for the RI change caused by particulate liquid water at elevated RH. In the current study, hygroscopicity was measured at dry sizes corresponding to $D_{p,em}$ of 150, 175, and 200 nm. Multiple RH sensors in the nafion tubes and OPCs controlled RHs to dry (<8%), 74%, 85%, and 92%, with RH uncertainty of 1.5%. Low particle loadings inherent in the marine atmosphere required increased on-line collection times at each DMA size step, but usually \leq one minute was sufficient to overcome counting statistic limitations. Overall uncertainty in GF calculations is 4.5%. Assuming particles to be uniform, non-light-absorbing spheres allows the assumption that the intensity of scattered light is a function of only RI and D_p . This assumption also allows calculation of dry, ‘effective’ RI from the known DMA-selected D_p and measured scattered light intensity.

2.4 Hygroscopic closure

A volume-weighted mixing rule was used to perform a hygroscopic closure using AMS and DASH-SP data, under the assumption of independent and additive water uptake by individual constituents in each particle:

$$GF_{\text{mixed}}(a_w) = \left(\sum_i \epsilon_i GF_i(a_w)^3 \right)^{1/3} \quad (1)$$

**Aerosol
hygroscopicity
closure using AMS
and DASH-SP data**

S. P. Hersey et al.

Title Page

Abstract

Introduction

Conclusions

References

Tables

Figures

⏪

⏩

◀

▶

Back

Close

Full Screen / Esc

Printer-friendly Version

Interactive Discussion

where GF_{mixed} is the overall particle GF , a_w is the water activity, GF_i is the hygroscopic growth factor for pure species i , and ϵ_i is the volume fraction of species i . At equilibrium, $a_w = RH$ (Seinfeld and Pandis, 2006). Values for ϵ_i were calculated for the following species, using AMS masses of ammonium (NH_4^+), nitrate (NO_3^-), sulfate (SO_4^{2-}), and total organic: ammonium nitrate (NH_4NO_3), ammonium sulfate ($(\text{NH}_4)_2\text{SO}_4$), ammonium bisulfate (NH_4HSO_4), sulfuric acid (H_2SO_4), and organic. Partitioning between sulfate species was determined on the basis of the ammonium to sulfate molar ratio. $(\text{NH}_4)_2\text{SO}_4$ is assumed to have a GF of unity at 74% since particles are exposed to RH well below its efflorescence point before subsequent rehumidification. The organic fraction was assumed to be hydrophilic WSOC, based on evidence of a high degree of organic oxygenation from AMS mass spectra (see Sect. 3.3). Values of GF_i for the organic fraction were calculated as those necessary to minimize the root mean square error in comparing predictions with measured hygroscopicity.

3 Results

GF values for seven flights (RF 7, 10, 11, 12, 13, 14, and 16) are presented in Table 2. Table 4 presents measured GF s at each RH and each $D_{p,\text{dry}}$. Typically, multiple measurements were made on each leg, at each size, for each flight. The error reported is \pm one standard deviation in these multiple measurements. When only one measurement was made at a given size in a given leg, it is reported without error. Ship plumes were encountered on flights 10 and 16, as evidenced by brief, significantly elevated particle number concentration. Analysis of GF measurements in these presumptive plumes is not presented in the present work.

3.1 Airmass origin

Relative to the other flights, RF 12 and 16 exhibited significantly suppressed water uptake at high RH for all dry sizes. During these two flights, 92% GF values for 200

**Aerosol
hygroscopicity
closure using AMS
and DASH-SP data**

S. P. Hersey et al.

Title Page

Abstract

Introduction

Conclusions

References

Tables

Figures

◀

▶

◀

▶

Back

Close

Full Screen / Esc

Printer-friendly Version

Interactive Discussion



nm $D_{p,dry}$ particles averaged 1.61 ± 0.14 , as compared with 1.91 ± 0.07 for all other flights. These low- GF flights corresponded to significantly elevated total organic, as measured by the AMS. Mass concentration averaged $1.97 \pm 1.71 \mu\text{g}/\text{m}^3$ organic (as opposed to $0.58 \pm 0.63 \mu\text{g}/\text{m}^3$ for all other flights), corresponding to volume fraction organic ($VF_{organic}$) of 0.46 ± 0.22 (as opposed to 0.24 ± 0.18 for all other flights).

Back-trajectory analysis suggests that the MASE-II flights can be categorized by air-mass origin as either clean/marine (flights 7, 10, 11, 13, 14) or polluted/continental (flights 12, 16). Figure 1 shows 92% GF measurements for 200 nm $D_{p,dry}$ particles, with corresponding 48-hr HYSPLIT (available at <http://www.arl.noaa.gov/ready/hysplit4.html>) back-trajectories identifying air-mass origin. Note that the low GF s and high $VF_{organic}$ measured on flights 12 and 16 correspond with air-mass origins over the continental United States, while higher GF s and lower $VF_{organic}$ measured on other flights correspond to air-mass origins over the clean marine environment. It is interesting to note that trajectories at sea level have marine origins for all flights, including low- GF flights 12 and 16, suggesting that aloft air-mass origin is a more significant factor in determining aerosol characteristics. Further, air-masses corresponding to clean, high- GF flights often pass either directly over or very near the San Francisco Bay Area, but these trajectories do not appear to significantly affect aerosol GF or $VF_{organic}$. It is also noteworthy that GF values at low RH were not significantly suppressed, with values of 1.31 ± 0.06 at 74% (compared with 1.31 ± 0.07 for all other flights). GF values at intermediate RH were moderately suppressed in the continental air-mass, measuring 1.53 ± 0.10 at 85% (compared with 1.58 ± 0.08 for all other flights). In other words, the effect of the high- $VF_{organic}$, polluted/continental air-mass is to significantly suppress GF at high RH, while having no measurable effect on aerosol water uptake at low RH and a moderate impact at intermediate RH.

3.2 Hygroscopicity trends

No size-dependent hygroscopicity was observed over the range of measured $D_{p,dry}$, despite slightly elevated $VF_{organic}$ at smaller sizes. This suggests that minor size-

dependent changes in composition had too small an impact on particle GF to be detected by the DASH-SP.

Figure 2 shows below- and corresponding above-cloud 92% GF values for all flights. There exists a ubiquitous trend of higher below-cloud aerosol GF values at high RH when compared with top of cloud hygroscopicity values (1.88 ± 0.14 below cloud, versus 1.78 ± 0.18 above cloud). Marker sizes, proportional to VF_{organic} suggest a trend of higher organic loading above cloud in several flights (0.27 ± 0.15 below cloud, versus 0.31 ± 0.21 above cloud). While variability is rather large in these measurements, the trend of elevated VF_{organic} above-cloud does correspond to suppressed GF at high RH. There is a trend of more moderate GF suppression at intermediate RH in the higher VF_{organic} above-cloud layer (1.53 ± 0.06 above cloud, as compared with 1.58 ± 0.07 below cloud). Unlike the continental-influenced flights, there is evidence of more significant suppression of low-RH GF s in above-cloud legs, with 74% GF values of 1.31 ± 0.05 above cloud, compared with 1.36 ± 0.05 below. It appears, then, that the elevated organic loadings typical of above-cloud legs are correlated with GF suppression at high RH, and more moderate GF suppression at lower RHs.

3.3 Hygroscopic closure

A hygroscopic closure was performed, using volume-weighted hygroscopic contributions from each chemical constituent identified by the AMS. O:C ratios for the flights presented were 0.92 ± 0.33 , with very similar ratios for below, above, and free troposphere legs on all flights. This result indicates a consistently uniform, highly oxidized organic component (Aiken et al., 2007), with little 'fresh,' or HOA-type organic carbon. With this evidence, the organic fraction was treated as a bulk, water-soluble constituent (Kondo et al., 2007), as opposed to being speciated into a soluble and insoluble OOA and HOA according to Zhang et al. (2005). As described in Sect. 2.4, GF values were calculated for the organic component of the aerosol by minimizing root mean square error when comparing measured GF s with volume-weighted closure predictions. Mission-averaged organic GF s were determined to be 1.20, 1.43, and 1.46 at

**Aerosol
hygroscopicity
closure using AMS
and DASH-SP data**

S. P. Hersey et al.

Title Page

Abstract

Introduction

Conclusions

References

Tables

Figures

⏪

⏩

◀

▶

Back

Close

Full Screen / Esc

Printer-friendly Version

Interactive Discussion

**Aerosol
hygroscopicity
closure using AMS
and DASH-SP data**

S. P. Hersey et al.

[Title Page](#)[Abstract](#)[Introduction](#)[Conclusions](#)[References](#)[Tables](#)[Figures](#)[⏪](#)[⏩](#)[◀](#)[▶](#)[Back](#)[Close](#)[Full Screen / Esc](#)[Printer-friendly Version](#)[Interactive Discussion](#)

74, 85, and 92% RH, respectively. These values agree well with those of hydrophilic multifunctional and dicarboxylic acids studied by Peng et al. (2001). Closure results are presented in Fig. 3. Markers in Fig. 3 are color-coded according to relative humidity, and marker size is proportional to VF_{organic} . The volume-weighted hygroscopic closure utilizing size-resolved AMS chemistry achieves good agreement with the 675 DASH-SP GF measurements, with an R^2 of 0.79. Agreement is better at lower values of RH, owing to smaller GF magnitudes and less overall GF variability.

Aside from the obvious RH dependence of GF values, the clearest trend in Fig. 3 is that of larger markers (higher VF_{organic}) at low GF transitioning to smaller markers (lower VF_{organic}) at high values of GF for the same RH. The clarity and regularity of this trend reveal the importance of the organic fraction in determining GF values, and suggest that, of all the chemical species considered in the closure, the organic fraction is a particularly crucial parameter in predicting GF .

3.4 Simplified parameterization

To further investigate the relative importance of each parameter in quantifying aerosol water uptake, and to determine the simplest statistical model still capable of accurately predicting GF , a backward stepwise linear regression was performed. The process, which eliminates predictors one-by-one to generate increasingly simplified linear representations of data, started with over 60 predictors, ranging from PILS and AMS chemical parameters to atmospheric data. The result is a two-parameter model that predicts GF as a function of RH and VF_{organic} :

$$GF = -0.314 + 2.33(\text{RH}) - 0.30(VF_{\text{organic}}) \quad (2)$$

Figure 4 demonstrates the accuracy with which this model predicts DASH-SP GF values over measured the range of RH and VF_{organic} . It is noteworthy that the R^2 for this model is 0.77, indicating that the simple, two-parameter model explains only 2% less variability than the full volume-weighted chemical closure, which contains significantly more information (i.e. multiple inorganic chemical species and their individual GF s, in

addition to organic fraction with its associated GF). So even with information on the specific nature of organics in the atmosphere, it appears as though accurate predictions of particle water uptake in the marine atmosphere can be made simply on the basis of relative humidity and the relative abundance of organics in the aerosol. While this model accurately predicts GF over the range of RH and VF_{organic} measured during MASE-II, it should not be used when RH is outside the range $74\% \leq \text{RH} \leq 92\%$, or where VF_{organic} is less than 0.1.

4 Discussion

Comparing mixed organic-inorganic particles with those comprised entirely of inorganic salts, there is a strong RH-dependence in the effect of organics on hygroscopicity (Peng et al., 2001). During the MASE-II field campaign, GF values at 74% RH averaged ~ 1.3 . Organic GF s were inferred to be 1.20 at 74% RH, suggesting that they contributed significantly to overall aerosol water uptake at low RH. GF values at 85% RH averaged ~ 1.6 during the campaign, and so the organic GF of 1.43 calculated for 85% RH suggests that organics played a less significant role, but still influenced water uptake at intermediate RH. An organic GF value of 1.46 was calculated for 92% RH, while 92% GF measurements averaged ~ 1.8 , suggesting that organics contributed little to overall GF at high RH.

Inorganic salts exhibit deliquescent behavior as RH is increased. Many organics do not deliquesce or crystallize when RH is increased or decreased, respectively, but instead retain water at RH values well below the RH of deliquescence (RHD) of the inorganic salts with which they often co-exist in ambient particles. As a result, at RH values below the salt RHD, the presence of organics enhances water uptake. Thus, the effect of organics is to contribute significantly to overall water uptake at low values of RH in mixed organic-inorganic particles. At high RH, on the other hand, organics tend to take up significantly less water than the inorganic constituents with which they co-exist in ambient particles. Therefore, at RH values above the inorganic RHD, organics

Aerosol hygroscopicity closure using AMS and DASH-SP data

S. P. Hersey et al.

Title Page

Abstract

Introduction

Conclusions

References

Tables

Figures

⏪

⏩

◀

▶

Back

Close

Full Screen / Esc

Printer-friendly Version

Interactive Discussion

appear to suppress water uptake relative to that which a pure inorganic particle would exhibit.

Figure 5 shows the behavior of a pure ammonium sulfate (AS) particle, pure organic acid (OA) particle, and a mixed organic acid and ammonium sulfate (OA/AS) particle over the range $50\% \leq RH \leq 94\%$. Note that the mixed OA/AS particle shows smooth growth with RH, as opposed to the deliquescent behavior exhibited by the pure AS particle. The tendency of organics to retain water at low RH causes water uptake behavior for the OA/AS particle to follow that of the descending (i.e. efflorescence) branch of the pure AS growth curve. Since pure OA takes up less water at high RH than does pure AS, the growth curve for the OA/AS particle is suppressed, compared with that of pure AS. The overall result, as predicted by thermodynamic theory, is that the presence of OA leads to enhanced water uptake at low RH and suppressed GF at high RH.

Virkkula et al. (1999) concluded that the most important factor contributing to GF suppression at high RH was the volume fraction of organic present in an aerosol. Others have suggested that the exact chemical identity of the organic constituents is not especially important, and that for an organic component classified as either oxidized or hydrocarbon-like, its relative abundance determines its effect on GF values (McFiggans et al., 2005; Moore and Raymond, 2008). Results presented here from a stepwise linear regression on GF data from the marine atmosphere suggest that the single most important factor in predicting GF (aside from RH) is, indeed, VF_{organic} .

In most instruments that measure aerosol hygroscopicity, residence times for humidification are on the order of seconds, much longer than the equilibration time for most inorganics with water vapor. Sjogren et al. (2007) noted, however, that particles with high volume fraction organic material may require as long as 40 s to achieve equilibrium with water vapor. If such long times are necessary to achieve equilibrium, hygroscopic measurement methods suitable for the field will tend to overpredict GF at low RH (water vapor does not evaporate completely from the particle during the drying process), while underpredicting GF at high RH (insufficient humidification time is

Aerosol hygroscopicity closure using AMS and DASH-SP data

S. P. Hersey et al.

Title Page

Abstract

Introduction

Conclusions

References

Tables

Figures

⏪

⏩

◀

▶

Back

Close

Full Screen / Esc

Printer-friendly Version

Interactive Discussion

provided for the organic fraction to achieve thermodynamic equilibrium with water vapor). In electrodynamic balance (EDB, (Cohen et al., 1987a,b,c)) studies, suspended particles are subjected to extended exposure to water vapor (minutes to hours), establishing equilibrium. Some organics exhibit extremely high deliquescence relative humidities (DRH) (e.g., oxalic acid), while others exhibit gradual hygroscopic growth at low RH and substantial growth at high RH (e.g., malonic acid) (Peng et al., 2001). It is possible, given the wide range of organic species in the atmosphere and correspondingly wide range of hygroscopic properties associated with those species, and the relatively short humidification times in the DASH-SP and other similar instruments, that the effects attributed to organics may reflect some kinetic instrumental limitations.

5 Conclusions

We report a hygroscopic closure study for the marine aerosol, using high-resolution AMS chemical data coupled with highly time-resolved, multiple-RH hygroscopicity measurements from the DASH-SP.

Airmasses originating from continental locations showed elevated organic loading, and corresponded to significant GF suppression at high RH. More moderate GF suppression was measured at intermediate RH and no impact was observed at low RH. A comparison of above-cloud with below-cloud aerosol indicated that a slightly organic-enriched layer above cloud corresponded with suppressed GF s at high RH. A volume-weighted hygroscopic closure provided excellent agreement with measured GF s, and mission-averaged organic GF s at 74, 85, and 92% were calculated to be 1.20, 1.43, and 1.46, respectively. These GF values are relatively high when compared with many previous estimations of organic GF , but agree well with values reported for dicarboxylic and multifunctional acids. These high organic GF s are indicative of the highly oxidized state of the aged organic fraction. A simplified parameterization for predicting GF was developed using a stepwise linear regression method. This parameterization is a function of only RH and VF_{organic} , and explains only 2% less variability than does

Aerosol hygroscopicity closure using AMS and DASH-SP data

S. P. Hersey et al.

Title Page

Abstract

Introduction

Conclusions

References

Tables

Figures

⏪

⏩

◀

▶

Back

Close

Full Screen / Esc

Printer-friendly Version

Interactive Discussion



the volume-weighted chemical closure. The GF predictions and parameterizations presented here accurately predict GF s from high-resolution chemical inputs, and may be broadly applicable to the marine environment, where some oxidized organics are present in an otherwise clean, atmosphere.

5 The richness of this hygroscopic/chemical data set underlies the significance of coupling the DASH-SP instrument with the AMS. The improved time resolution available with the DASH-SP eliminates much of the time-averaging of AMS chemical data that is otherwise necessary with less highly time-resolved HTDMA hygroscopicity measurements. The importance of simultaneous GF measurements at multiple RH values is demonstrated by a simplified parameterization for predicting GF as a function of RH and VF_{organic} ; a result potentially important for efficiently representing aerosol-water interactions in global models.

15 *Acknowledgements.* This work was supported by the Office of Naval Research grant N00014-04-1-0118. We acknowledge the committed, meticulous work of the CIRPAS Twin Otter crew, especially pilot Mike Hubbell and copilot Chris McGuire.

References

- Aiken, A. C., DeCarlo, P. F., and Jimenez, J. L.: Elemental analysis of organic species with electron ionization high-resolution mass spectrometry, *Anal. Chem.*, 79, 8350–8358, 2007. 16798
- 20 Ansari, A. S. and Pandis, S. N.: Water absorption by secondary organic aerosol and its effect on inorganic aerosol behavior, *Environ. Sci. Technol.*, 34, 71–77, 2000. 16791
- Carrico, C. M., Rood, M. J., and Ogren, J. A.: Aerosol light scattering properties at Cape Grim, Tasmania, during the First Aerosol Characterization Experiment (ACE 1), *J. Geophys. Res.*, 103, 16 565–16 574, 1998. 16791
- 25 Carrico, C. M., Rood, M. J., Ogren, J. A., Neususs, C., Wiedensohler, A., and Heintzenberg, J.: Aerosol optical properties at Sagres, Portugal during ACE-2, *Tellus Series B-Chemical and Physical Meteorology*, 52, 694–715, 2000. 16791
- Choi, M. Y. and Chan, C. K.: Continuous measurements of the water activities of aqueous

Aerosol hygroscopicity closure using AMS and DASH-SP data

S. P. Hersey et al.

Title Page

Abstract

Introduction

Conclusions

References

Tables

Figures

◀

▶

◀

▶

Back

Close

Full Screen / Esc

Printer-friendly Version

Interactive Discussion

- droplets of water-soluble organic compounds, *J. Phys. Chem. A*, 106, 4566–4572, 2002a. 16791
- Choi, M. Y. and Chan, C. K.: The effects of organic species on the hygroscopic behaviors of inorganic aerosols, *Environ. Sci. Technol.*, 36, 2422–2428, 2002b. 16791
- 5 Clegg, S. L. and Seinfeld, J. H.: Thermodynamic models of aqueous solutions containing inorganic electrolytes and dicarboxylic acids at 298.15 K. 2. Systems including dissociation equilibria, *J. Phys. Chem. A*, 110, 5718–5734, 2006. 16791, 16817
- Cocker, D. R., Clegg, S. L., Flagan, R. C., and Seinfeld, J. H.: The effect of water on gas-particle partitioning of secondary organic aerosol. Part I: alpha-pinene/ozone system, *Atmos. Environ.*, 35, 6049–6072, 2001a. 16791
- 10 Cocker, D. R., Mader, B. T., Kalberer, M., Flagan, R. C., and Seinfeld, J. H.: The effect of water on gas-particle partitioning of secondary organic aerosol: II. m-xylene and 1,3,5-trimethylbenzene photooxidation systems, *Atmos. Environ.*, 35, 6073–6085, 2001b. 16791
- Cohen, M. D., Flagan, R. C., and Seinfeld, J. H.: Studies of concentrated electrolyte-solutions using the electrodynamic balance. 1. Water activities for single-electrolyte solutions, *J. Phys. Chem.*, 91, 4563–4574, 1987a. 16802
- 15 Cohen, M. D., Flagan, R. C., and Seinfeld, J. H.: Studies of concentrated electrolyte-solutions using the electrodynamic balance. 2. Water activities for mixed-electrolyte solutions, *J. Phys. Chem.*, 91, 4575–4582, 1987b. 16802
- 20 Cohen, M. D., Flagan, R. C., and Seinfeld, J. H.: Studies of concentrated electrolyte-solutions using the electrodynamic balance. 3. Solute nucleation, *J. Phys. Chem.*, 91, 4583–4590, 1987c. 16802
- Cruz, C. N. and Pandis, S. N.: Deliquescence and hygroscopic growth of mixed inorganic-organic atmospheric aerosol, *Environ. Sci. Technol.*, 34, 4313–4319, 2000. 16791
- 25 Dougle, P. G., Veefkind, J. P., and ten Brink, H. M.: Crystallisation of mixtures of ammonium nitrate, ammonium sulphate and soot, *J. Aerosol Sci.*, 29, 375–386, 1998. 16791
- Drewnick, F., Jayne, J. T., Canagaratna, M., Worsnop, D. R., and Demerjian, K. L.: Measurement of ambient aerosol composition during the PMTACS-NY 2001 using an aerosol mass spectrometer. Part II: Chemically speciated mass distributions, *Aerosol. Sci. Tech.*, 38, 104–117, suppl. 1, 2004a. 16793
- 30 Drewnick, F., Schwab, J. J., Jayne, J. T., Canagaratna, M., Worsnop, D. R., and Demerjian, K. L.: Measurement of ambient aerosol composition during the PMTACS-NY 2001 using an aerosol mass spectrometer. Part I: Mass concentrations, *Aerosol. Sci. Tech.*, 38, 92–103,

**Aerosol
hygroscopicity
closure using AMS
and DASH-SP data**

S. P. Hersey et al.

[Title Page](#)[Abstract](#)[Introduction](#)[Conclusions](#)[References](#)[Tables](#)[Figures](#)[⏪](#)[⏩](#)[◀](#)[▶](#)[Back](#)[Close](#)[Full Screen / Esc](#)[Printer-friendly Version](#)[Interactive Discussion](#)

suppl. 1, 2004b. 16793

Duplissy, J., Gysel, M., Alfara, M. R., Dommen, J., Metzger, A., Prevot, A. S. H., Weingartner, E., Laaksonen, A., Raatikainen, T., Good, N., Turner, S. F., McFiggans, G., and Baltensperger, U.: Cloud forming potential of secondary organic aerosol under near atmospheric conditions, *Geophys. Res. Lett.*, 35, L03818, doi:10.1029/2007GL031075, 2008. 16791

Gysel, M., Crosier, J., Topping, D. O., Whitehead, J. D., Bower, K. N., Cubison, M. J., Williams, P. I., Flynn, M. J., McFiggans, G. B., and Coe, H.: Closure study between chemical composition and hygroscopic growth of aerosol particles during TORCH2, *Atmos. Chem. Phys.*, 7, 6131–6144, 2007, <http://www.atmos-chem-phys.net/7/6131/2007/>. 16792

Hameri, K., Charlson, R., and Hansson, H. C.: Hygroscopic properties of mixed ammonium sulfate and carboxylic acids particles, *AIChE J.*, 48, 1309–1316, 2002. 16791

Hegg, D. A., Covert, D. S., Crahan, K. K., Jonsson, H. H., and Liu, Y.: Measurements of aerosol size-resolved hygroscopicity at sub and supermicron sizes, *Geophys. Res. Lett.*, 33, L21808, doi:10.1029/2006GL026747, 2006. 16791

IPCC: Climate Change 2007: The Physical Science Basis. Contribution of Working Group I to the Fourth Assessment Report of the Intergovernmental Panel on Climate Change, Cambridge University Press, Cambridge, United Kingdom and New York, NY, USA, 2007. 16791

Jayne, J. T., Leard, D. C., Zhang, X. F., Davidovits, P., Smith, K. A., Kolb, C. E., and Worsnop, D. R.: Development of an aerosol mass spectrometer for size and composition analysis of submicron particles, *Aerosol. Sci. Tech.*, 33, 49–70, 2000. 16792

Kasten, F.: Visibility forecast in phase of pre-condensation, *Tellus*, 21(5), 631–635, 1969. 16809

Kim, J., Yoon, S. C., Jefferson, A., and Kim, S. W.: Aerosol hygroscopic properties during Asian dust, pollution, and biomass burning episodes at Gosan, Korea in April 2001, *Atmos. Environ.*, 40, 1550–1560, 2006. 16791

Kondo, Y., Miyazaki, Y., Takegawa, N., Miyakawa, T., Weber, R. J., Jimenez, J. L., Zhang, Q., and Worsnop, D. R.: Oxygenated and water-soluble organic aerosols in Tokyo, *J. Geophys. Res.*, 112, D01203, doi:10.1029/2006JD007056, 2007. 16798

Kreisberg, N. M., Stolzenburg, M. R., Hering, S. V., Dick, W. D., and McMurry, P. H.: A new method for measuring the dependence of particle size distributions on relative humidity, with application to the Southeastern Aerosol and Visibility Study, *J. Geophys. Res.*, 106, 14 935–14 949, 2001. 16791

**Aerosol
hygroscopicity
closure using AMS
and DASH-SP data**

S. P. Hersey et al.

Title Page

Abstract

Introduction

Conclusions

References

Tables

Figures

⏪

⏩

◀

▶

Back

Close

Full Screen / Esc

Printer-friendly Version

Interactive Discussion

**Aerosol
hygroscopicity
closure using AMS
and DASH-SP data**

S. P. Hersey et al.

[Title Page](#)[Abstract](#)[Introduction](#)[Conclusions](#)[References](#)[Tables](#)[Figures](#)[⏪](#)[⏩](#)[◀](#)[▶](#)[Back](#)[Close](#)[Full Screen / Esc](#)[Printer-friendly Version](#)[Interactive Discussion](#)

- Lu, M. L., Conant, W. C., Jonsson, H. H., Varutbangkul, V., Flagan, R. C., and Seinfeld, J. H.: The Marine Stratus/Stratocumulus Experiment (MASE): Aerosol-cloud relationships in marine stratocumulus, *J. Geophys. Res.*, 112, D10209, doi:10.1029/2006JD007985, 2007. 16793
- 5 Magi, B. I. and Hobbs, P. V.: Effects of humidity on aerosols in southern Africa during the biomass burning season, *J. Geophys. Res.*, 108, 8495, doi:10.1029/2002JD002144, 2003. 16791
- Malm, W. C., Day, D. E., Kreidenweis, S. M., Collett, J. L., Carrico, C., McMeeking, G., and Lee, T.: Hygroscopic properties of an organic-laden aerosol, *Atmos. Environ.*, 39, 4969–4982, 2005. 16792
- 10 Massling, A., Leinert, S., Wiedensohler, A., and Covert, D.: Hygroscopic growth of sub-micrometer and one-micrometer aerosol particles measured during ACE-Asia, *Atmos. Chem. Phys.*, 7, 3249–3259, 2007, <http://www.atmos-chem-phys.net/7/3249/2007/>. 16791
- 15 McFiggans, G., Alfarra, M. R., Allan, J., Bower, K., Coe, H., Cubison, M., Topping, D., Williams, P., Decesari, S., Facchini, C., and Fuzzi, S.: Simplification of the representation of the organic component of atmospheric particulates, *Faraday Discuss.*, 130, 341–362, 2005. 16801
- Moore, R. H. and Raymond, T. M.: HTDMA analysis of multicomponent dicarboxylic acid aerosols with comparison to UNIFAC and ZSR, *J. Geophys. Res.*, 113, D04206, doi:10.1029/2007JD008660, 2008. 16791, 16801
- 20 Peng, C., Chan, M. N., and Chan, C. K.: The hygroscopic properties of dicarboxylic and multi-functional acids: Measurements and UNIFAC predictions, *Environ. Sci. Technol.*, 35, 4495–4501, 2001. 16791, 16799, 16800, 16802
- Peng, C. G. and Chan, C. K.: The water cycles of water-soluble organic salts of atmospheric importance, *Atmos. Environ.*, 35, 1183–1192, 2001. 16791
- 25 Petters, M. D., Kreidenweis, S. M., Snider, J. R., Koehler, K. A., Wang, Q., Prenni, A. J., and Demott, P. J.: Cloud droplet activation of polymerized organic aerosol, *Tellus Series B-Chemical and Physical Meteorology*, 58, 196–205, 2006. 16791
- Prenni, A. J., DeMott, P. J., Kreidenweis, S. M., Sherman, D. E., Russell, L. M., and Ming, Y.: The effects of low molecular weight dicarboxylic acids on cloud formation, *J. Phys. Chem. A*, 30, 105, 11 240–11 248, 2001. 16791
- Prenni, A. J., De Mott, P. J., and Kreidenweis, S. M.: Water uptake of internally mixed particles containing ammonium sulfate and dicarboxylic acids, *Atmos. Environ.*, 37, 4243–4251, 2003.

16791

Prenni, A. J., Petters, M. D., Kreidenweis, S. M., DeMott, P. J., and Ziemann, P. J.: Cloud droplet activation of secondary organic aerosol, *J. Geophys. Res.*, 112, D10223, doi:10.1029/2006JD007963, 2007. 16791

5 Rood, M. J., Larson, T. V., Covert, D. S., and Ahlquist, N. C.: Measurement of laboratory and ambient aerosols with temperature and humidity controlled nephelometry, *Atmos. Environ.*, 19, 1181–1190, 1985. 16791

Saathoff, H., Naumann, K. H., Schnaiter, M., Schock, W., Mohler, O., Schurath, U., Weingartner, E., Gysel, M., and Baltensperger, U.: Coating of soot and $(\text{NH}_4)_2\text{SO}_4$ particles by ozonolysis products of alpha-pinene, *J. Aerosol Sci.*, 34, 1297–1321, 2003. 16791

10 Seinfeld, J. and Pandis, S.: *Atmospheric Chemistry and Physics*, Second Edition, Wiley-Interscience, New York, NY, USA, 2006. 16796

Sjogren, S., Gysel, M., Weingartner, E., Baltensperger, U., Cubison, M. J., Coe, H., Zardini, A. A., Marcolli, C., Krieger, U. K., and Peter, T.: Hygroscopic growth and water uptake kinetics of two-phase aerosol particles consisting of ammonium sulfate, adipic and humic acid mixtures, *J. Aerosol Sci.*, 38, 157–171, 2007. 16791, 16801

Sorooshian, A., Hersey, S., Brechtel, F., Corless, A., Flagan, R., and Seinfeld, J.: Rapid, Size-Resolved Aerosol Hygroscopic Growth Measurements: Differential Aerosol Sizing and Hygroscopicity Spectrometer Probe (DASH-SP), *Aerosol. Sci. Tech.*, 42, 445–464, 2008. 16794

20 Topping, D. O., McFiggans, G. B., and Coe, H.: A curved multi-component aerosol hygroscopicity model framework: Part 1 – Inorganic compounds, *Atmos. Chem. Phys.*, 5, 1205–1222, 2005a. 16791

Topping, D. O., McFiggans, G. B., and Coe, H.: A curved multi-component aerosol hygroscopicity model framework: Part 2 – Including organic compounds, *Atmos. Chem. Phys.*, 5, 1223–1242, 2005b. 16791

25 Varutbangkul, V., Brechtel, F. J., Bahreini, R., Ng, N. L., Keywood, M. D., Kroll, J. H., Flagan, R. C., Seinfeld, J. H., Lee, A., and Goldstein, A. H.: Hygroscopicity of secondary organic aerosols formed by oxidation of cycloalkenes, monoterpenes, sesquiterpenes, and related compounds, *Atmos. Chem. Phys.*, 6, 2367–2388, 2006, <http://www.atmos-chem-phys.net/6/2367/2006/>. 16791

30 Virkkula, A., Van Dingenen, R., Raes, F., and Hjorth, J.: Hygroscopic properties of aerosol formed by oxidation of limonene, alpha-pinene, and beta-pinene, *J. Geophys. Res.*, 104, 3569–3579, 1999. 16791, 16801

ACPD

8, 16789–16817, 2008

**Aerosol
hygroscopicity
closure using AMS
and DASH-SP data**

S. P. Hersey et al.

Title Page

Abstract

Introduction

Conclusions

References

Tables

Figures

⏪

⏩

◀

▶

Back

Close

Full Screen / Esc

Printer-friendly Version

Interactive Discussion

Zhang, Q., Alfarra, M. R., Worsnop, D. R., Allan, J. D., Coe, H., Canagaratna, M. R., and Jimenez, J. L.: Deconvolution and quantification of hydrocarbon-like and oxygenated organic aerosols based on aerosol mass spectrometry, *Environ. Sci. Technol.*, 39, 4938–4952, 2005. 16792

ACPD

8, 16789–16817, 2008

**Aerosol
hygroscopicity
closure using AMS
and DASH-SP data**

S. P. Hersey et al.

Title Page

Abstract

Introduction

Conclusions

References

Tables

Figures

◀

▶

◀

▶

Back

Close

Full Screen / Esc

Printer-friendly Version

Interactive Discussion

16808



Table 1. Previous marine aerosol hygroscopicity studies.

Investigators	Year	Study Area	Reported GF_s
Hegg	1996	Eastern Pacific	1.4–2.0
Berg	1998	Pacific and Southern Oceans	1.56–1.78
Kotchenruther	1999	Mid-Atlantic	1.81–2.3 ^a
Gasso	2000	Eastern Atlantic	$\gamma=0.51-0.75^b$
Swietlicki	2000	Northeastern Atlantic	1.6–1.8
Zhou	2001	Arctic Ocean	1.4–1.9
Hegg	2002	Eastern Pacific	$\gamma=0.2 - -0.7^b$
Vakeva	2002	Northeastern Atlantic	1.3–1.4 ^c
Massling	2003	Atlantic and Indian Oceans	1.6–2.0
Hegg	2006	Eastern Pacific	1.3–1.5
Kaku	2006	Eastern Pacific	1.2–1.7
Tomlinson	2007	Southeastern Pacific	1.3–1.7 ^d

^a Ratio of light scattering coefficient at 80% RH to 30% RH.

^b γ from the expression $b_{sp}(RH)/b_{sp}(RH_0) = ((1 - RH/100)/(1 - RH_0/100))^{-\gamma}$ (Kasten, 1969).

^c Aitken mode particles.

^d 85% RH.

Aerosol hygroscopicity closure using AMS and DASH-SP data

S. P. Hersey et al.

Title Page

Abstract

Introduction

Conclusions

References

Tables

Figures

◀

▶

◀

▶

Back

Close

Full Screen / Esc

Printer-friendly Version

Interactive Discussion

Aerosol hygroscopicity closure using AMS and DASH-SP data

S. P. Hersey et al.

Title Page

Abstract

Introduction

Conclusions

References

Tables

Figures

⏪

⏩

◀

▶

Back

Close

Full Screen / Esc

Printer-friendly Version

Interactive Discussion

Table 2. MASE-II flights.

Flight Number (RF)	Date	Type of Flight
1	10-Jul-07	Cloud/aerosol interactions
2	11-Jul-07	Cloud/aerosol interactions
3	12-Jul-07	Bovine source probe
4	14-Jul-07	Cloud/aerosol interactions
5	15-Jul-07	Cloud/aerosol interactions
6	16-Jul-07	Coordinated ship plume probe
7	21-Jul-07	Cloud/aerosol interactions
8	22-Jul-07	Cloud/aerosol interactions
9	23-Jul-07	Cloud/aerosol interactions
10	24-Jul-07	Cloud/aerosol interactions
11	25-Jul-07	Cloud/aerosol interactions
12	26-Jul-07	Cloud/aerosol interactions
13	28-Jul-07	Cloud/aerosol interactions
14	29-Jul-07	Cloud/aerosol interactions
15	30-Jul-07	Bovine source probe
16	31-Jul-07	Cloud/aerosol interactions

Table 3. MASE-II instrument payload.

Parameter	Instrument	Time Resolution	Detection Limit	Size Range
Particle Number Concentration	Condensation Particle Counter (TSI CPC 3010)	1 s	0–10 000 cm ⁻³	$D_p \geq 10$ nm
Particle Number Concentration (including ultrafine)	Condensation Particle Counter (TSI CPC 3025)	1 s	0–100 000 cm ⁻³	$D_p \geq 3$ nm
Aerosol Size Distribution	Scanning differential mobility analyzer (Dual Automated Classified Aerosol Detector, DACAD)	73 s	N/A	10–700 nm
Aerosol Size Distribution	Passive Cavity Aerosol Spectrometer Probe (PCASP)	1 s	N/A	0.1–2.6 μ m
Separation of Cloud Droplets From Interstitial Aerosol	Counterflow Virtual Impactor	N/A	N/A	N/A
Cloud Droplet Size Distribution	Phase Doppler Interferometer (PDI)	1 s	N/A	4–200 μ m
Cloud and Drizzle Drop Size Distribution	Forward Scattering Spectrometer Probe (FSSP)	1 s	N/A	1–46 μ m
Cloud Droplet Liquid Water Content	Light Diffraction (Gerber PVM-100 probe)	1 s	N/A	5–50 nm
Aerosol Bulk Ionic Composition and Soluble Organic Composition	Particle-Into-Liquid Sampler (PILS)	5 min	0.02–0.28 μ g/m ³	1 μ m
Aerosol Bulk Composition (non-refractory species)	Aerodyne Time-of-Flight Aerosol Mass Spectrometer (TOF-AMS)	1 s or 15 s	0.25 μ g/m ³	40 nm $\leq D_{p,va} \leq 1$ μ m
Aerosol Hygroscopicity	Differential Aerosol Sizing and Hygroscopicity Spectrometer Probe (DASH-SP)	15 - 100 s	N/A	150 nm $\leq D_p \leq 1$ μ m
Soot Absorption	Photoacoustic Absorption Spectrometer (PAS)	1 s	1 Mm ⁻¹	10 nm–5 μ m
Soot Absorption	Particle Soot Absorption Photometer (PSAP)	≥ 1 s	N/A	N/A

Aerosol hygroscopicity closure using AMS and DASH-SP data

S. P. Hersey et al.

Title Page

Abstract

Introduction

Conclusions

References

Tables

Figures

⏪

⏩

◀

▶

Back

Close

Full Screen / Esc

Printer-friendly Version

Interactive Discussion

Table 4. *GF* results for below, above, free troposphere (FT), and ship plume measurements.

150 nm												
Flight	Below			Above			FT			Ship Plume		
	74%	85%	92%	74%	85%	92%	74%	85%	92%	74%	85%	92%
7	1.40±0.04	1.57±0.03	1.82±0.05	1.26±0.06	1.55±0.04	1.78±0.01	1.40±0.03	1.55±0.03	1.84±0.04			
10	1.42±0.04	1.60±0.06	1.80±0.04	1.37±0.10	1.57±0.04	1.71±0.11	1.42±0.03	1.56±0.04	1.70±0.07	1.42±0.04	1.62±0.03	1.78±0.04
11	1.44±0.05	1.61±0.06	1.80±0.07	1.40±0.07	1.51±0.02	1.64±0.05	1.38±0.07	1.52±0.06	1.65±0.10			
12	1.38±0.03	1.58±0.03	1.63±0.04	1.34±0.04	1.51±0.03	1.55±0.01	1.38±0.02	1.60±0.01	1.63±0.01			
13	1.39±0.01	1.61±0.05	1.82±0.02	1.35±0.01	1.61±0.03	1.75±0.05	1.27±0.05	1.49±0.07	1.61±0.08			
14	1.36±0.05	1.65±0.21	1.82±0.14	1.39±0.02	1.62±0.01	1.87±0.09	1.37±0.03	1.60±0.03	1.77±0.06			
16	1.41±0.02	1.58±0.05	1.64±0.08	1.33±0.03	1.52±0.03	1.54±0.03	1.29±0.04	1.49±0.07	1.52±0.06	1.38±0.02	1.59±0.02	1.61±0.04

175 nm												
Flight	Below			Above			FT			Ship Plume		
	74%	85%	92%	74%	85%	92%	74%	85%	92%	74%	85%	92%
7	1.36±0.06	1.54±0.02	1.95±0.03	1.28±0.04	1.53±0.03	1.91±0.06	1.24±0.08	1.52±0.03	1.87±0.10			
10	1.41±0.06	1.59±0.05	1.93±0.02	1.34±0.05	1.51±0.01	1.83±0.06	1.33±0.02	1.60±0.03	1.89±0.05	1.34±0.02	1.55±0.05	1.88±0.06
11	1.31±0.08	1.48±0.07	1.82±0.09	1.31±0.03	1.44±0.09	1.77±0.03	1.33±0.04	1.53±0.12	1.77±0.23			
12	1.33±0.02	1.55±0.04	1.63±0.08	1.26±0.06	1.48±0.08	1.51±0.07	1.35±0.02	1.57±0.01	1.60±0.01			
13	1.34±0.03	1.58±0.04	2.00±0.05	1.3	1.55	1.78	1.24±0.05	1.44±0.06	1.63±0.10			
14	1.34±0.01	1.63±0.02	2.03±0.01	1.32±0.02	1.58±0.02	1.91±0.05	1.33±0.02	1.50±0.08	1.79±0.22			
16	1.35±0.04	1.54±0.03	1.62±0.06	1.28±0.02	1.43±0.04	1.45±0.04	1.24±0.04	1.38±0.06	1.40±0.10	1.33±0.03	1.52±0.04	1.55±0.03

200 nm												
Flight	Below			Above			FT			Ship Plume		
	74%	85%	92%	74%	85%	92%	74%	85%	92%	74%	85%	92%
7	1.37±0.04	1.57±0.03	1.98±0.03	1.22±0.06	1.56±0.05	1.92±0.0.01	1.21±0.01	1.54±0.08	1.91±0.04			
10	1.41±0.09	1.72±0.09	2.01±0.05	1.33±0.02	1.57±0.07	1.87±0.04	1.35±0.01	1.63±0.06	1.93±0.06	1.33±0.04	1.66±0.06	1.95±0.05
11	1.25±0.11	1.45±0.17	1.86±0.07	1.26	1.47	1.83	1.36±0.16	1.56±0.15	1.89±0.20			
12	1.33±0.03	1.64±0.03	1.73±0.05	1.29±0.03	1.48±0.10	1.55±0.12	1.37±0.05	1.64±0.05	1.69±0.04			
13	1.36±0.05	1.68±0.05	2.01±0.04	1.3	1.61	1.85	1.21±0.08	1.45±0.07	1.78±0.12			
14	1.42±0.11	1.65±0.05	1.98±0.10	1.3±0.05	1.60±0.03	1.96±0.01	1.35±0.09	1.59±0.10	1.89±0.11			
16	1.35±0.02	1.59±0.05	1.77±0.08	1.26±0.02	1.45±0.08	1.53±0.10	1.23±0.06	1.40±0.10	1.40±0.11	1.33±0.03	1.62±0.04	1.66±0.06

Aerosol hygroscopicity closure using AMS and DASH-SP data

S. P. Hersey et al.

Title Page

Abstract

Introduction

Conclusions

References

Tables

Figures

⏪

⏩

◀

▶

Back

Close

Full Screen / Esc

Printer-friendly Version

Interactive Discussion

Aerosol hygroscopicity closure using AMS and DASH-SP data

S. P. Hersey et al.

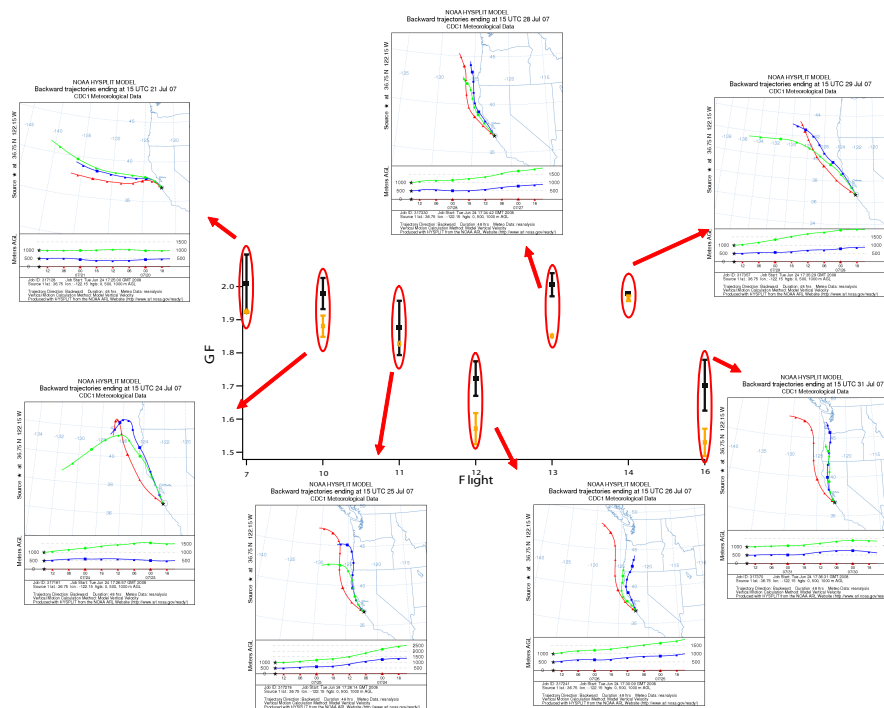


Fig. 1. 92% GF values for 200 nm particles are shown as below and above cloud flight legs. 48-hr HYSPLIT back-trajectories show air mass origin for each flight. Flights 12 and 16 show both suppressed GF values and continental, polluted air mass origin.

Title Page

Abstract

Introduction

Conclusions

References

Tables

Figures

◀

▶

◀

▶

Back

Close

Full Screen / Esc

Printer-friendly Version

Interactive Discussion

Aerosol
hygroscopicity
closure using AMS
and DASH-SP data

S. P. Hersey et al.

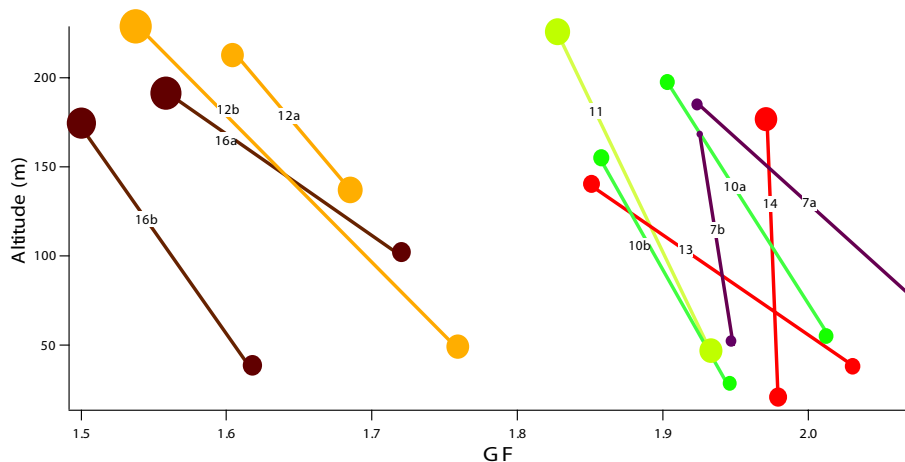


Fig. 2. Below- and above-cloud 92% GF values for 200 nm particles as a function of altitude, with lines connecting measurements made on the same “trip” from bottom to top of cloud. Marker size is proportional to VF_{organic} . “a” and “b” designate separate “trips” during the same flight.

[Title Page](#)[Abstract](#)[Introduction](#)[Conclusions](#)[References](#)[Tables](#)[Figures](#)[◀](#)[▶](#)[◀](#)[▶](#)[Back](#)[Close](#)[Full Screen / Esc](#)[Printer-friendly Version](#)[Interactive Discussion](#)

Aerosol
hygroscopicity
closure using AMS
and DASH-SP data

S. P. Hersey et al.

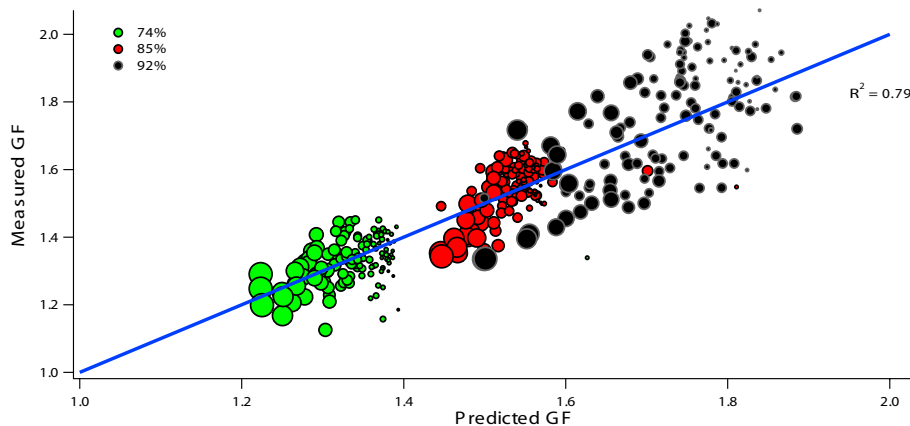


Fig. 3. Measured GF values versus volume-weighted predictions. Markers are color-coded with RH, and marker size is proportional to $V_{F_{\text{organic}}}$, as determined by the AMS. The blue line represents 1:1.

[Title Page](#)[Abstract](#)[Introduction](#)[Conclusions](#)[References](#)[Tables](#)[Figures](#)[◀](#)[▶](#)[◀](#)[▶](#)[Back](#)[Close](#)[Full Screen / Esc](#)[Printer-friendly Version](#)[Interactive Discussion](#)

Aerosol
hygroscopicity
closure using AMS
and DASH-SP data

S. P. Hersey et al.

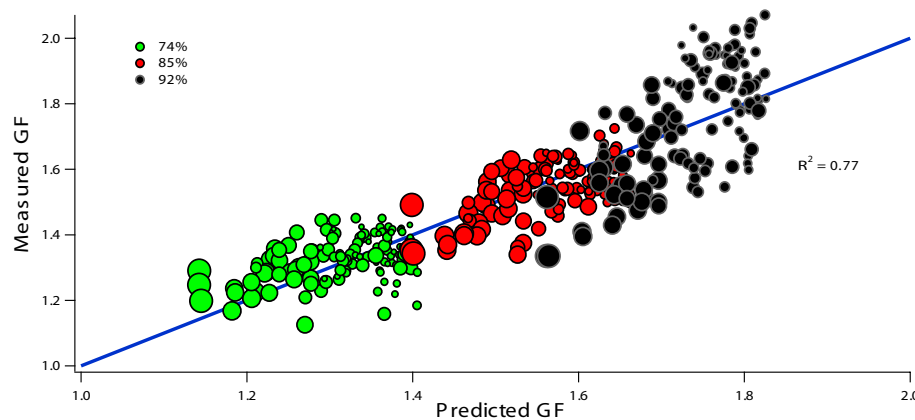


Fig. 4. Predictions of GF from the simplified parameterization. Markers are color-coded with RH, and marker size is proportional to VF_{organic} , as determined by the AMS. The blue line represents 1:1.

[Title Page](#)[Abstract](#)[Introduction](#)[Conclusions](#)[References](#)[Tables](#)[Figures](#)[◀](#)[▶](#)[◀](#)[▶](#)[Back](#)[Close](#)[Full Screen / Esc](#)[Printer-friendly Version](#)[Interactive Discussion](#)

**Aerosol
hygroscopicity
closure using AMS
and DASH-SP data**

S. P. Hersey et al.

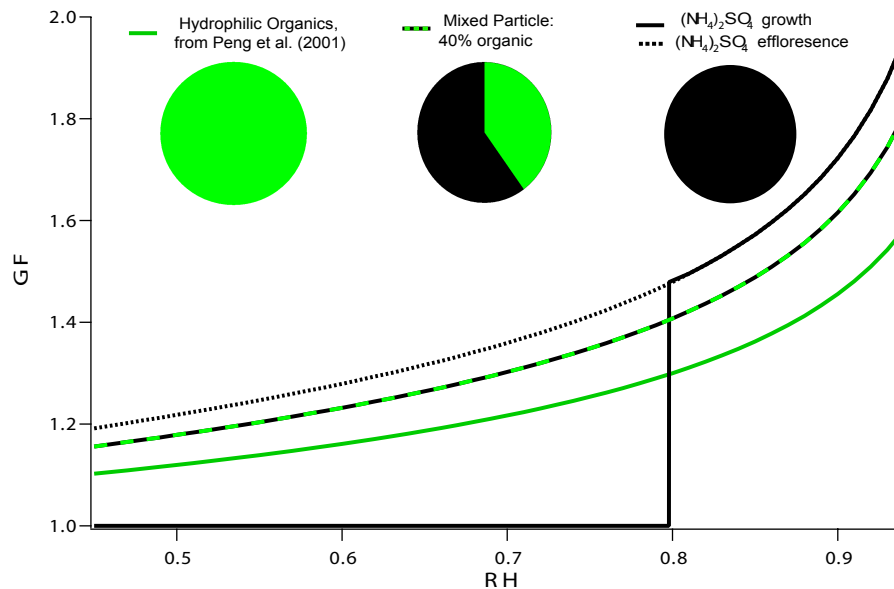


Fig. 5. Comparison of growth curves for pure ammonium sulfate, pure hydrophilic organic, and mixed organic/inorganic particles. Ammonium sulfate curves calculated from AIM (Clegg and Seinfeld, 2006).

[Title Page](#)[Abstract](#)[Introduction](#)[Conclusions](#)[References](#)[Tables](#)[Figures](#)[⏪](#)[⏩](#)[◀](#)[▶](#)[Back](#)[Close](#)[Full Screen / Esc](#)[Printer-friendly Version](#)[Interactive Discussion](#)